Relationship of dayside auroral precipitations to the open-closed separatrix and the pattern of convective flow

Article

Published Version

www.reading.ac.uk/centaur

CentAUR

Central Archive at the University of Reading

Reading's research outputs online

Relationship of dayside auroral precipitations to the open-closed separatrix and the pattern of convective flow

M. Lockwood

Rutherford Appleton Laboratory, Chilton, England, United Kingdom

Abstract. The implications are discussed of acceleration of magnetospheric ions by reflection off two magnetopause Alfvén waves, launched by the reconnection site into the inflow regions on both sides of the boundary. The effects of these waves on the ion populations, predicted using the model described by *Lockwood et al.* [1996], offer a physical interpretation of all the various widely used classifications of precipitation into the dayside ionosphere, namely, central plasma sheet, dayside boundary plasma sheet (BPS), void, low-latitude boundary layer (LLBL), cusp, mantle, and polar cap. The location of the open-closed boundary and the form of the convection flow pattern are discussed in relation to the regions in which these various precipitations are typically found. Specifically, the model predicts that both the LLBL and the dayside BPS precipitations are on newly opened field lines and places the convection reversal within the LLBL, as is often observed. It is shown that this offers solutions to a number of paradoxes and problems that arise if the LLBL and BPS precipitations are thought of as being on closed field lines. This model is also used to make quantitive predictions of the longitudinal extent and latitudinal width of the cusp, as a function of solar wind density.

1. Introduction

Equatorward of the cusp precipitation of magnetosheath-like plasma into the dayside auroral ionosphere, an energized magnetospheric population, termed "dayside boundary plasma sheet" (BPS), can often be observed [*Newell et al.*, 1991a]. An interesting example is given in Plate 1 of *Pinnock et al.* [1993], which shows data from an equatorward pass by the DMSP - F9 satellite through the southern - hemisphere cusp near noon. This pass took place during an interval of southward interplanetary magnetic field (IMF), with a negative B_y component. The precipitation is classified according to the definitions used by *Newell and Meng* [1992], namely, "polar cap", "mantle", "cusp", "low-latitude boundary layer", LLBL, "boundary plasma sheet", BPS, "central plasma sheet", CPS, and "void". This example illustrates that the cusp precipitation is in a region of strong westward flow, consistent with the tension force on newly - opened field lines [*Cowley*, 1981]. This "Svalgaard-Mansurov" effect is just one of the many pieces of evidence showing that the cusp is on newly opened field lines, as recently reviewed by *Lockwood and Smith* [1994] and as demonstrated by the successful modeling of the precipitation spectra by *Onsager et al.* [1993] and by *Lockwood and Davis* [1996] for magnetopause reconnection which is steady and pulsed in rate respectively.

For other satellite passes, a similar ion precipitation feature equatorward of the cusp has been classed as LLBL (see second example in Plate 1 of *Newell and Meng* [1994a]). The LLBL, in general terms, contains a mixture of magnetosphere-like and magnetosheath-like plasmas. The difference between the LLBL and BPS classifications is discussed by *Newell et al.* [1991a] and often rests on the electron characteristics. Thus locations where the ions are as in the LLBL but the electrons are more similar to the CPS would be classed as dayside BPS by these authors. Often these two classes are deliberately combined [e.g., *de la Beaujardiere et al.*, 1993] or have been classified differently by different authors (see discussion by *Woch and Lundin* [1993]).

A key general point that needs to be addressed here relates to the significance of all the various low-altitude precipitation regions. *Vasyluinas* [1979] considered the ionospheric precipitation regions to be the field-aligned projections of magnetospheric source regions, and they are usually given the same names as a result. The classification scheme discussed above is largely based upon this philosophy because, as part of its derivation, spectra at low altitudes were compared with those at high altitudes. Thus, for example, *Newell and Meng* [1992] regarded their map of the ionospheric regions as a map of the magnetosphere. Note that the magnetospheric populations are usually defined by the fluxes outside the loss cone, whereas most particles seen at low altitudes are within the loss cone. In addition, *Lockwood and Smith* [1993] point out that this philosophy neglects magnetospheric convection and particle motion in the crossed electric and magnetic fields. The convection electric field means that although particles move along magnetic field lines, during their time of flight the field line onto which they are frozen will have convected. (Note, however, that this effect in no way relies on the (approximate) frozen-in theorem used here to describe it: an entirely equivalent description can be made in terms of particle motion in crossed electric and magnetic fields.) Thus the trajectories are not field-aligned and depend on the energy and pitch angle of the particle. Indeed, this is the very basis of the observed

velocity filter effects [*Reiff et al.*, 1977]. Thus not only does a spectrum of particle energies from one point in the magnetosphere map to a spread of locations in the ionosphere, but also, a spread of energies seen at any one point (at a fixed pitch angle) in the ionosphere maps to a spread of source locations in the magnetosphere. Similarly, the spread of source locations is evidenced by the spread in pitch angles at any one energy. As discussed below, this effect is highly significant for low-energy magnetosheath-like ions. It is also significant for electrons in that, although high-energy electrons do have much smaller flight times and thus much more field-aligned trajectories, the fluxes of electrons are somehow modified by those of the ions in order to maintain quasi-neutrality [*Burch*, 1985]. This means that any classification scheme which depends on the fluxes of either ions or electrons, or both, is subject to strong influence by this effect.

In this paper, we pay particular attention to the dayside BPS and LLBL which, in many of the cases presented [e.g., *Pinnock et al.*, 1993; *Newell and Meng*, 1994a; *Kremser et al.*, 1995], are revealed to share the same velocity-filter dispersion ramp as the cusp. This strongly suggests that the generation and transport of both dayside BPS and LLBL ions are intimately linked with that of the cusp ions. The dayside BPS and LLBL contain ions with energies elevated well above those of the shocked solar wind plasma in the magnetosheath (up to over the 30 keV limit of the ion instrument in the above examples). Acceleration of sheath ions occurs when they cross the magnetopause current sheet by flowing along newly - opened field lines, as is well explained by the theory of *Cowley* [1982]. This theory has been highly successful, not only in predicting the ion distribution functions seen at the dayside magnetopause [*Smith and Rodgers*, 1991; *Fuselier et al.*, 1991, *Gosling et al.*, 1990b] but also in predicting the cusp, mantle, and polar cap precipitations of magnetosheath-like ions resulting from either quasi-steady [*Onsager et al.*, 1993; *Lockwood et al.*, 1994] or pulsed [*Lockwood and Davis*, 1996] magnetopause reconnection. The use of the ion acceleration theory in these models has been discussed in detail by *Lockwood* [1995a]. However, the acceleration predicted by *Cowley* [1982] is not adequate to explain the high fluxes of the most energetic BPS/LLBL ions. For example, the open magnetosphere models of the cusp by *Onsager et al.* [1993], *Lockwood and Smith* [1994], and *Lockwood and Davis* [1996] all give a plateau of peak ion energies (with detectable fluxes) of only 7 to 10 keV.

Consequently, several alternative ideas have been proposed to explain the energetic BPS/LLBL ions. *Newell and Meng* [1992] regard the dayside BPS as an extension of nightside BPS, implying that the ions are accelerated on newly closed field lines in the tail, as initially implied by *Vasyliunas* [1979]. *Alem and Delcourt* [1995] suggested an explanation in terms of chaotic orbits in a closed field - line magnetic cusp topology. However, neither of these ideas can produce ions with an energy dispersion that is continuous with that of the ions in the cusp region, which is clearly the case for several observed examples [*Newell et al.*, 1991b; *Pinnock et al.*, 1993; *Newell and Meng*, 1994a]. In addition, the closed magnetic cusp topology invoked by Alem and Delcourt is not consistent with the cusp precipitation seen poleward of the BPS on open field lines. *Curran and Goertz* [1989] considered chaotic ion orbits within a reconnection layer; however, a simpler and more effective description has recently been supplied by *Lockwood et al.* [1996] using a simple generalization of the theory by *Cowley* [1982] to explain both the BPS and LLBL ions in terms of the

open magnetospheric model. Lockwood et al. invoke acceleration by reflection of magnetospheric ions off two Alfvén waves, launched by the reconnection site into the inflow regions where plasma flows toward the reconnecting magnetopause. The "interior" wave stands in the inflow on the magnetospheric side of the boundary, whereas the "exterior" Alfvén wave stands in the inflow on the magnetosheath side. The majority of the field rotation takes place at the exterior wave, and so this is the main magnetopause current sheet. The interior wave is the inner edge of the reconnection layer (also called the open LLBL), and its existence can be inferred from the fact that the field in the LLBL has a slightly different orientation to that of closed field lines in the magnetosphere proper [*Cowley et al.*, 1983; *Hapgood and Bryant*, 1992]. Lockwood et al. have shown that the effect of the interior wave is to produce accelerated ions which are continuous in their dispersion with the magnetosheath ions injected along the newly opened field lines and seen in the LLBL and cusp precipitation regions at low altitudes. These authors were able to make a very good match to the case originally presented by *Newell et al.* [1991b] (and which has, incidentally, been the subject of a great many of the other studies mentioned above: specifically, *Onsager et al.* [1993], *Lockwood et al.* [1994], and *Alem and Delcourt* [1995] which all discussed this one example). *Lockwood and Moen* [1996] have applied the theory of *Lockwood et al.* [1996], to explain another example of BPS and LLBL ions, as reported by *Moen et al.* [1996]. The importance of the interior Alfvén wave is that its speed is much higher than that of the exterior wave, owing to the lower plasma density on the magnetospheric side of the boundary. Reflection off this faster wave generates more highly accelerated ions, and detectable fluxes at 30 keV and over can be achieved.

The schematics by *Newell and Meng* [1992, 1994a] show where the various dayside precipitations typically occur, based on their survey of dayside ion and electron observations and as defined by their classification scheme. The relationship of some of these precipitations to the open-closed magnetic separatrix and the pattern of ionospheric convection (and thus the associated pattern of field aligned currents) was considered theoretically by *Cowley et al.* [1991a] for strongly southward IMF ($B_z \ll 0$) with a large IMF $|B_y|$. However, the origin of the BPS was not considered; instead, these authors paid particular attention to the location of the "cusp" field-aligned currents (also called the "region 0" or "mantle" currents) on open field lines associated with the large $|B_y|$ component of the interplanetary magnetic field (IMF). These predictions were found to be consistent with observations by *de la Beaujardiere et al.* [1993]. However, this physical interpretation does not cover all cases. For example, when the IMF is southward ($B_z < 0$) and $|B_y|$ is small, a symmetric pattern about noon is expected [*Ohtani et al.*, 1995b]. If $|B_y|$ is large but B_z is positive or close to zero, a lobe circulation cell may be added [*Ohtani et al.*, 1995a]. Much of the debate in the above papers relates to the location and extent of the cusp field-aligned currents and the variations with the IMF orientation. This paper is not concerned with this aspect; rather, we wish to discuss the origins of the ion populations, and the location and extent of the region in which each is found. To do this, we here restrict our attention to the simplest case of strongly southward IMF *($B_z < 0$)* and $|B_y| \approx$ 0. In doing so, we provide answers to some important outstanding questions and problems that are discussed in sections 2 and 3.

2. Are LLBL Field Lines Open or Closed?

The open magnetosphere model predicts that the precipitation at low altitudes evolves from cusp to mantle and then to polar cap as the field line evolves over the magnetopause away from the reconnection site and into the tail lobe [Reiff et al., 1977; Cowley et al., 1991b; Lockwood and Smith, 1993, 1994; Onsager et al., 1993; Lockwood, 1995a]. This evolution is seen in full along the flow streamlines in the steady state case and thus may sometimes be seen if the satellite follows the flow streamline quite closely. Recently, several authors have suggested the low-altitude LLBL precipitation is also on open field lines [e.g., Lockwood and Smith, 1993; Lyons et al., 1994; Moen et al., 1996].

At the magnetopause current sheet (the exterior Alfvén wave), application of tangential stress-balance tests to particle and field data [e.g., Paschmann et al., 1986; Sonnerup et al., 1990] reveals that there is a layer of accelerated magnetosheath plasma, mixed with magnetospheric plasma, which is formed by the two populations flowing along newly opened field lines at the local Alfvén speed in the rest frame of the field lines (i.e., the Whalén relation is found to apply). Other observations (specifically, of the directions of the accelerated flows [Gosling et al., 1990a], of the form of their ion distribution functions [Smith and Rodgers, 1991; Fuselier et al., 1991], and of electron and ion edges due to time-of-flight dispersion effects [Gosling et al., 1990b]) leave no reasonable doubt that this "reconnection layer" or "LLBL" is on newly opened field lines. However, there is no direct evidence that this open LLBL at the magnetopause is directly related to the precipitation classed as LLBL in the topside ionosphere. Hill and Reiff [1977] and Woch and Lundin [1992] have shown that the cusp ion energies increase in the low-altitude velocity-filter dispersion ramp to energies above those in the magnetosheath, providing evidence that the highest - energy ions of the accelerated ion flows at the magnetopause do, indeed, appear in the ionosphere close to the magnetic separatrix. The models of Onsager et al. [1993], Lockwood and Smith [1994], and Lockwood [1995a] stress the role of the velocity filter effect and show that the precipitations at any one point in the ionosphere arise from a spread of locations on the magnetopause. Allowance for this must be made when considering the origin of the LLBL. Lockwood and Smith [1993] used realistic boundary-tangential field line velocities over the magnetopause to show that the spread of magnetopause source locations supplying ions to one point in the ionosphere was very large, being of the order of 10-20 Earth radii (R_E). This being the case, the ionospheric LLBL cannot be equated with a magnetopause LLBL in the manner inherent in the work of Newell and Meng [1992] and Lyons et al. [1994]. Newell and Meng [1993] argued that the spread of source locations is not so large as to invalidate this association and cite the model of Onsager et al. [1993] as showing this. However, this model did not allow for the effect of the draping of the IMF in the magnetosheath which results in the model field lines evolving over the magnetopause at speeds much lower than those that are found by application of the stress-balance test to data from the dayside magnetopause [e.g. Paschmann et al., 1986; Sonnerup et al., 1990; Smith and Rodgers, 1991]. To compensate for this, Onsager et al. raised the de-Hoffman Teller frame velocities employed in the computation of the particle acceleration (T.G. Onsager, private communication, 1996). As a result, realistic particle spectra were obtained, but the spreads of source locations (and the

steady state ionospheric flow speeds) were underestimated. The modeling by Lockwood [1995a] uses a simple, fixed sheath field draping and predicts that source location spreads are large, as estimated by Lockwood and Smith [1993] from typical boundary-tangential field line speeds at the magnetopause.

Other magnetopause observations, showing a mixture of magnetosheath-like and magnetosphere-like plasmas on northward pointing field lines, have been interpreted as an LLBL on closed field lines [Eastman and Hones, 1979; Eastman et al., 1976; Mitchell et al., 1987; Traver et al., 1991; Lotko and Sonnerup, 1995]. That these field lines are genuinely closed is not certain because the use of particle distributions to infer the magnetic topology is notoriously difficult. This is because of the effects of particle flight times and of magnetic mirrors on open field lines [Scholer et al., 1982; Daly and Fritz, 1982; Cowley and Lewis, 1990]. In addition, unlike the open LLBL, the mechanisms responsible for introducing magnetosheath plasma into a closed LLBL are not clear. Sonnerup [1980] pointed out that the observed waves were not adequate to drive the required cross-field diffusion, a finding confirmed by later studies [Owen and Slavin, 1992; Winske et al., 1995; Treumann et al., 1995]. Nishida [1989] proposed a mechanism whereby reconnection may be responsible for plasma populations on a closed LLBL when the IMF points northward. He invoked highly patchy reconnection such that field lines opened at one reconnection site were reclosed at a later time elsewhere. During the time that the field line was open, magnetosheath plasma was free to flow in and magnetosphere plasma was free to flow out, giving the observed plasma mixture. Recently, Song and Russell [1992] proposed a similar mechanism, but involving only two large-scale reconnection sites, poleward of the cusps. Numerical simulations by Richard et al. [1994] indicate that magnetosheath plasma could, indeed, get onto closed field lines in this way.

3. Dayside Precipitation, the Pattern of Convection, and the Open-Closed Field Line Boundary

The debate about the magnetic topology within the LLBL at the magnetopause certainly has implications for the precipitation classed as LLBL at low altitudes, even though the relationship between the two is not simple. Figure 1 contrasts two possible relationships of the dayside precipitation regions (shaded according to the code bar) to the ionospheric convection streamlines (thin lines with arrows) and to the open-closed boundary (thick line). The open/closed boundary is dashed where magnetic flux is transferred across it (i.e., at the "merging" gap which maps to the magnetopause reconnection X - line) and is solid where it is not (i.e., an "adiaroic" segment, meaning "not flowing across" [Siscoe and Huang, 1985]). The key difference between the two plots in Figure 1 is the location of the open-closed field line boundary and, in particular, the consequent topology of field lines within the ionospheric LLBL and BPS regions. Both cases are drawn for the steady state limit, with strongly southward interplanetary magnetic field (B_z < 0) which has no major dawn-dusk component ($B_y \approx 0$). Figure 1 could readily be adapted to non steady situations, for example, during the growth phases of a substorm when the polar cap is expanding and the adiaroic segments of the boundary migrate equatorward [Siscoe and Huang, 1985; Cowley and Lockwood, 1992] and/or for large IMF |B_y| , [Cowley et al., 1991b, a].
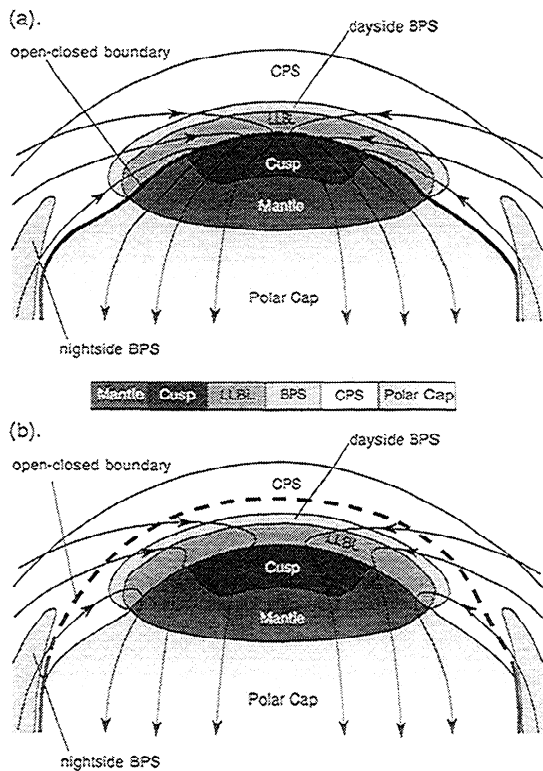
Figure 1. Two schematic views showing possible relationships of the regions of dayside precipitations (shaded as given by the code bar), the open-closed field line boundary (shown as a solid thick line where it is "adiaroic" and as a dashed thick line at the merging gap) and the pattern of convection (streamlines are thin lines with arrows): (a) a closed low-latitude boundary layer (LLBL) and (b) an open LLBL.

In Figure 1a, the LLBL and BPS precipitations are on closed field lines, whereas in Figure 1b they are on open. The regions of precipitation are broadly as sketched by *Newell and Meng* [1992, 1994a]; however, the region near noon between the CPS and the LLBL, which they characterized as typically being "void", has not been included. This has been done because void can occur when and where the flux falls below the one-count level, which depends on the instrument geometric factor (and thus its sensitivity threshold) as much as on the geophysical conditions. From the occurrence frequency of the void classification, it is clear that it usually arises because either the BPS and/or CPS fluxes are below the one-count level. In addition, *Newell and Meng* [1994a] are careful to note that the void region between the CPS and LLBL is often not devoid of precipitation but that the precipitation present cannot be easily identified with any of the other classifications. The occurrence frequency plots by *Newell and Meng* [1992; 1994a] show that the minimum occurrence probability of BPS is around noon but is of the order of 25%, and, indeed, the examples given by *Pinnock et al.* [1993], *de la Beaujardiere et al.* [1993], and *Ohtani et al.* [1995a, b] all show precipitation classed as BPS close to noon. Consequently, we here reclassify the void region near noon (between CPS and LLBL) as being part of the dayside BPS which therefore extends across all magnetic local time (MLT) around noon. We will discuss later why there are passes for which the noon BPS, as defined here, is classed as void in the surveys of *Newell and Meng* [1992, 1994a].

In Figure 1a, the open-closed boundary is at the boundary between cusp and LLBL, whereas in Figure 1b it is farther

equatorward than this and lies near the poleward edge of the CPS. Some differences and implications of these two patterns are discussed in sections 3.1-3.4 below.

3.1. Extent of the Precipitation Regions in MLT

The statistical results of *Newell and Meng* [1992; 1994a] show the cusp precipitation occurrence to cover a relatively small range of MLT (about 3 hours), compared to the mantle and LLBL which both cover about 7 hours. This has been reflected in Figure 1. In Figure 1a, the narrow cusp extent is set by the length of the merging gap and the LLBL, being on closed field lines and populated by a different mechanism, does not share this extent. However, the results of Newell and Meng indicate that the LLBL has roughly the same length in MLT as the mantle on open field lines. This has to be attributed to coincidence in Figure 1a. On the other hand, in Figure 1b the widths of the LLBL and the mantle both reflect the MLT extent of the merging gap, but it is not immediately apparent what sets the smaller longitudinal extent of the cusp.

3.2. Speed and Pattern of Convection in the Cusp

Another difference between Figures 1a and 1b relates to the poleward flow speeds in the cusp and the reconnection voltage. The observed transpolar voltage and its dependence on the orientation of the IMF show that magnetopause reconnection produces a voltage of the order of 110 kV when the IMF points strongly southward [e.g., *Cowley*, 1984]. If the cusp represents the location of newly opened field lines and if the LLBL is closed, then all the flow streamlines in the polar cap must first channel though a narrow constriction, often referred to as the "throat" [*Heelis et al.*, 1976], as in Figure 1a. This requires a voltage of the order of 110 kV across the cusp and, for the longitudinal width of 1000 km suggested by the statistics of *Newell and Meng* [1992, 1994a], a poleward flow speed through the cusp of the order of 2 km s^{-1}. Such a speed is somewhat higher than is typically observed for this component of the cusp flow, as is reflected in average models of the convection pattern [e.g., *Heppner and Maynard*, 1987; *Shue and Weimer*, 1994]. Poleward flow speeds of less than 1 km s^{-1} are also typical of case studies of the cusp region: for example, *Baker et al.* [1997] have recently studied a period when the transpolar voltage (determined by the assimilated mapping of ionospheric electrodynamics (AMIE) technique from magnetometer network data) was about 60 kV, during which the poleward flow speed in the cusp was 0.5 km s^{-1}. For an interval studied by *Lockwood et al.* [1993], the transpolar voltage was near 100 kV, yet the poleward flow speed in the cusp was still near 0.5 km s^{-1}. In addition, the throat flow pattern is not often seen. Rather, the flow pattern tends to show a broad convection reversal throughout the dayside as reported by *Jørgensen et al.* [1984] and reproduced in the statistical models of the convection pattern (see discussion by *Lockwood* [1991]). As shown in Figure 1b, the broader region of flow reversal into the polar cap is consistent with the idea that the LLBL is not closed but rather that it is on the most recently opened field lines. The extent of the LLBL of the order of 2000 km implied by the statistics of *Newell and Meng* [1992, 1994a] gives a more reasonable poleward plasma speed of 1 km s^{-1} for the transpolar voltage of 110 kV.

This discussion about reconnection voltage and flow speeds in the cusp has often taken on extreme forms. For example, *Stasiewicz* [1991] argued that the cusp was so small that almost

any reconnection voltage in the magnetopause surface led to unrealistically large flows in the cusp ionosphere. This author used a Tsyganenko magnetic field model (which has virtually no open flux threading the dayside magnetopause) and superposed a uniform IMF to generate some open flux. However, this practice neglects the draping of the IMF in the magnetosheath and, as a result, underestimates the total amount of open flux threading the dayside magnetopause (and the corresponding size of the precipitation region at the foot of those newly opened field lines in the ionosphere). In addition, non steady situations like substorm growth phases (when the rate at which open flux is produced by magnetopause reconnection rate greatly exceeds the rate at which it is destroyed by tail reconnection) or magnetopause erosion events (when the dayside reconnection produces open flux much more rapidly than the solar wind can transport it into the tail) can produce even more flux threading the dayside magnetopause than is expected in steady state. *Crooker et al.* [1991] have modeled the increase in the longitudinal extent of the ionospheric cusp with increasing reconnection voltage, an increase which means that flow speeds do not become excessively large. If one equates the cusp precipitation region extent with the length of the merging gap e.g., [*Newell and Meng*, 1994a], the model of Crooker et al. overestimates the extent of the cusp. The difference between the longitudinal extents of the cusp and the merging gap is discussed in section 7 of the present paper.

3.3. Meaning of the Boundaries Between Regions

There are also problems with the concept of boundaries between these precipitation regions, when we allow for convection. The particle trajectories in the crossed electric and magnetic fields give the velocity filter effect and the well-known energy-latitude and energy-pitch angle dispersions. The many observations of such dispersions show that ions, in the main, move adiabatically and without scatter under the influence of these fields. This means that the particles seen by a satellite at any one point originate from a spread of locations downstream from the observation site [*Lockwood and Smith*, 1993]. The source locations for any two precipitation regions in the ionosphere must therefore overlap, and the field-aligned divider between them does not simply extend into the magnetosphere because of the convection electric field.

For example, consider the low-altitude LLBL/cusp boundary shown in Figure 2. Two trajectories of ions seen at a point C within the cusp region are shown. These are for the ions with the maximum and minimum energy of field-parallel motion which can be detected by the satellite at C. If C is close to the LLBL/cusp boundary, the ions seen at C must all have originated downstream and thus on field lines, the ionospheric foot of which is classed as LLBL. This being the case, the open-closed boundary could, potentially, be at the LLBL-cusp border, as in Figure 1a. However, this must mean that the cusp ions seen at C all originated downstream on closed field lines in the magnetosphere and subsequently found themselves on open field lines as reconnection opened their field line during their time of flight from the magnetopause and the ionosphere. Thus placing the open-closed boundary at the LLBL/cusp interface is inconsistent with the open magnetosphere model of the cusp particle entry. Alternatively, if the cusp particles are injected across the magnetopause along open field lines, as is predicted by the highly successful open magnetosphere model, much or all of the low-altitude LLBL immediately equatorward of the
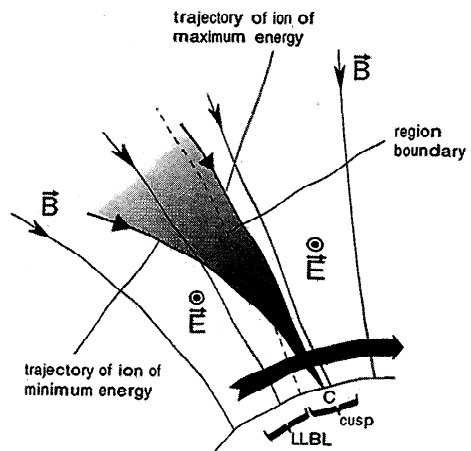
Figure 2. Schematic showing the trajectories of cusp ions to a single point C in the region of the ionosphere where the precipitation is classed as cusp. The trajectories are for the ions seen at C with the maximum and minimum energies of field-parallel motion, and so the shaded region is the source for the spectrum seen at C. The dashed line is the field-aligned projection of the boundary between the low-altitude LLBL and cusp precipitation regions.

cusp must also be on open field lines [*Lockwood and Smith*, 1993].

3.4. Location of the Electron Edge

The electron edge [*Gosling et al.*, 1990b] would be seen just poleward of the LLBL-cusp boundary in Figure 1a, whereas in Figure 1b it is near the CPS-BPS border. At the electron edge, a satellite flying from closed to open field lines notes a loss of high-energy, field-aligned, magnetospheric (CPS) electrons for the first time: these are lost by flowing out along the newly opened field lines through the magnetopause. Very shortly thereafter lower-energy magnetosheath-like electrons, flowing in the opposite direction, are seen for the first time. However, fluxes of the incoming sheath electrons are somehow restricted by the slower ions, so that charge neutrality is maintained [*Burch*, 1985]. Low-altitude observations often reveal the energetic CPS electrons very clearly, and when they are seen, their loss is evident and is equatorward of the LLBL and near the CPS-BPS border, as discussed by *Lockwood et al.* [1996]: this can also be seen, for example, in Figure 2 of *Watermann et al.* [1993]; Plates 1 and 3 of *Newell et al.* [1991a]; Plates 1a-1c of *de la Beaujardiere et al.* [1993]; and Plates 1, 3, and 4 of *Ohtani et al.* [1995b]. This feature is sometimes referred to as the trapping boundary [e.g., *Nishida et al.*, 1993] and is never, by definition of the LLBL, poleward of the LLBL. Thus, if we associate this observed feature (on the dayside) with the electron edge discussed by *Gosling et. al.* [1990b], its ionospheric location calls for the situation in Figure 1b and thus Figure 1a cannot apply.

4. Prediction of Ion Precipitation Spectra

Figure 3 shows the ion distribution function in the immediate vicinity of the X line which was modeled by *Lockwood et al.* [1996] and was the best fit to the cusp observations presented by *Newell et al.* [1991b]. The phase space density is grey-scaled as a function of velocity parallel and perpendicular to the magnetic field, with positive parallel velocities being away from the magnetopause and toward the ionosphere. The largest
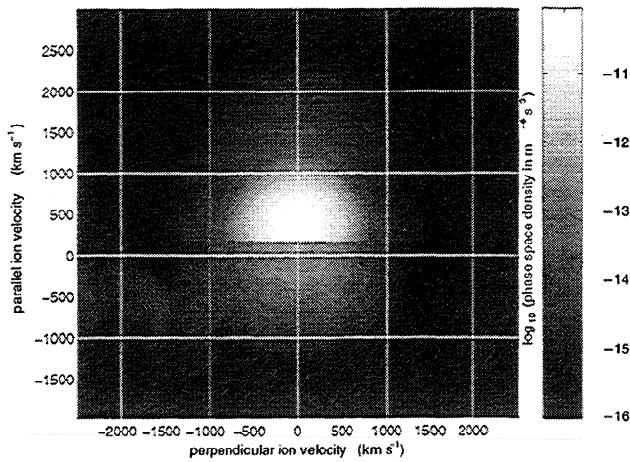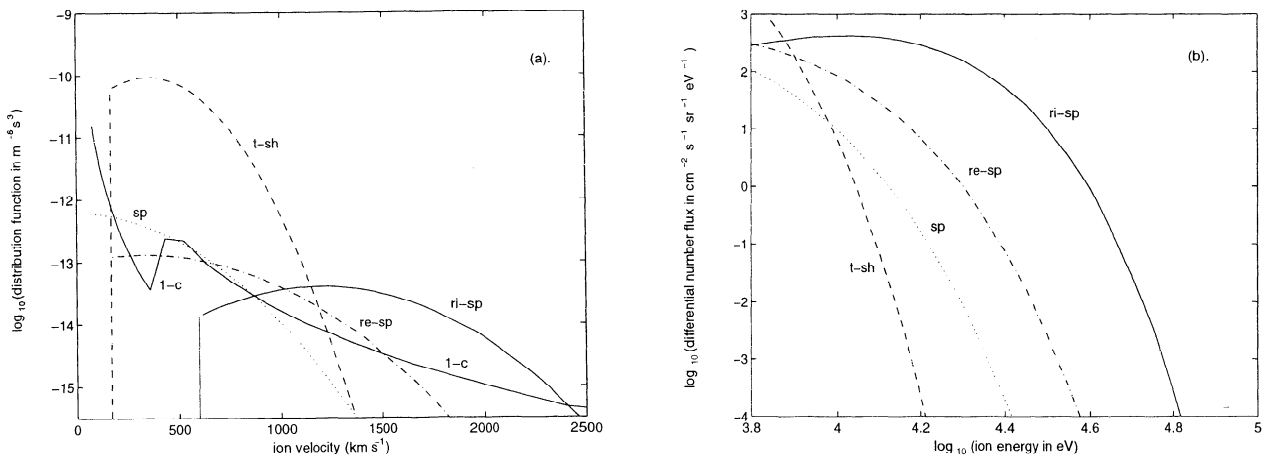
Figure 3. Modeled distribution function of ions at the magnetopause (near ion edge and near X line) predicted by *Lockwood et al.* [1996]. This population would be seen close to the reconnection site and between the magnetic separatrix and the interior Alfvén wave. The populations are listed in the field-parallel slice of this distribution shown in Figure 4a. The conditions at the magnetopause are as given in the caption of Figure 4.

phase-space densities reveal the D-shaped distribution of injected magnetosheath ions (termed the "t-sh" population by Lockwood et al.), as predicted by *Cowley* [1982]. This population has a low velocity cut off at the speed with which field lines move over the magnetopause in the outflow region from the X line (here 168 km s^{-1}). The fitting of the data to define this lower-energy, sheath-like ion population was described by *Lockwood et al.* [1994]. The populations flowing toward the magnetopause are the magnetospheric ions ("sp") which were present on closed field lines prior to reconnection. The populations seen flowing toward the Earth with high velocities are sp ions which have been reflected off the interior

or exterior Alfvén waves ("ri-sp" and "re-sp," respectively). The parameters which were adjusted by *Lockwood et al.* [1996] to produce the best fit hot population were the reflection factor r_b a heating factor on reflection h_i, and the speed of the interior wave (here 600 km s^{-1}). The values required to fit other observed examples may be considerably different; however, this set does provide a general framework by which other cusp passes can be understood, as discussed below for the midaltitude pass presented by *Kremser et al.* [1995]. The best fit populations produced from these best fit parameters can be seen more clearly in Figure 4a which shows the field parallel segment of the $f(v)$ shown in Figure 3. In Figure 4, another population ("re-sp") can be seen. These are originally sp ions which have traveled through the interior wave and then been reflected off the exterior wave. The lower solid line (labeled "1-c") is the one-count level of a typical DMSP ion detector. The caption of Figure 4 lists all the inputs to the computation of the distribution function, which are similar to those derived by *Lockwood et al.* [1996]. Because the ions in Figure 4 are all of zero pitch angle, they are the ones which will precipitate into the ionosphere, without mirroring in the converging magnetic field.

As mentioned above, in order to understand the generality of these predictions, it is useful to compare these model fits with data for a different cusp pass by a different (midaltitude) satellite, as presented by *Kremser et al.* [1995] (hereafter referred to as KEA). To do so, Figure 4b shows the differential energy flux ("intensity") spectra corresponding to the high-energy part of Figure 4a (using the same coding and labeling scheme), on the same scales as were used by KEA in their Figure 6. From KEA's Figure 6a it can be seen that, whereas the sp population corresponds to the population they term ring current, the re-sp and/or ri-sp population offers a broad explanation of what they term "boundary region 1" which clearly contains ions which are energized to above ring current levels. Thus the model agrees with KEA's suggestion that their


Figure 4. (a) Modeled field-parallel segments of the distribution function at the X line of magnetospheric ion populations: t-sh is the transmitted magnetosheath population (dashed line); sp is the magnetospheric population on closed field lines (dotted line) which gives the re-sp population (dotted-dashed line) when reflected off the exterior RD and gives ri-sp (solid line) when reflected off the interior RD. The t-sh population has a density and temperature of 1.2×10^7 m^{-3} and 4.9×10^6 K; respectively, the sp population has a density of 4.3×10^5 m^{-3} and a temperature of 1.5×10^7 K, all values relating to the field-parallel direction. The Alfvén speed on the magnetospheric side of the boundary is 600 km s^{-1} and on the magnetosheath side of the boundary is 190 km s^{-1} where the field-aligned sheath velocity is -22 km s^{-1}. The density reflection factors for the sp population at the exterior and interior RDs are $r_e = 0.2$ and $r_i = 0.03$, and the corresponding field-parallel heating factors are $h_e = 1.2$ and $h_i = 1.3$. The solid line marked 1-c is the one-count level of the ion detector on the DMSP-F7 satellite. (b). The corresponding intensity spectra at high energies.

"boundary region 1" is generated by interaction of magnetospheric ions with the magnetopause; however, it is not clear if it is the interior or the exterior Alfvén wave that is involved. The average spectrum shown by KEA for this region is consistent with acceleration of the ring current spectrum by reflection off an Alfvén wave moving at 300 km s^{-1}. This value could apply to the interior but is possibly more typical of the exterior wave and so these observations do not confirm that the ri-sp population is present in addition to the re-sp. KEA's boundary region 1 spectrum would be consistent with a low energy time-of-flight cutoff of the ri-sp and/or re-sp ions of about E_{ic} = 20 keV (below which only sp ions are seen): thus, for example, for a reconnection site which is a distance d of 20 R_E from the satellite, this corresponds to a time elapsed since reconnection of $(t_s\text{-}t_o) = (1/d) (2E_{ic}/m)^{1/2} = 65$ s (t_s is the time that a field line is observed and t_o is the time that it was opened by reconnection). After this time, E_{ic} will drop below 20 keV, and the hot tail of the injected sheath population (t-sh) will be seen, giving what KEA term "boundary region 2": in KEA's Figure 6b this region would be seen when E_{ic} < 10 keV which, for the example d of 20 R_E used above, corresponds to $(t_s\text{-}t_o)$ > 92 s. At still greater $(t_s\text{-}t_o)$, the re-sp population will not be present and the t-sh ions will be classed as cusp, evolving to mantle, as shown in Figure 6c of KEA. That the ion populations evolve between the regions, in the way predicted by the model, is confirmed by the spectrogram (KEA's Figure 2) showing both the energy-latitude and energy-pitch angle dispersions. KEA also find that the ratios of the abundances of the species in each population are also consistent with the magnetosheath and magnetospheric origins of the populations, as predicted by the model.

Figure 5 shows the precipitating spectrum that results from the source population of field-aligned ions shown in Figure 4. The plot shows the differential energy flux, as a function of elapsed time since reconnection $(t_s\text{-}t_o)$, for the assumed d of 20 R_E. The $(t_s\text{-}t_o) = 0$ axis is the open-closed boundary, and the whole region shown $(t_s\text{-}t_o > 0)$ is on open field lines. To generate Figure 5, a convolution of the source characteristics
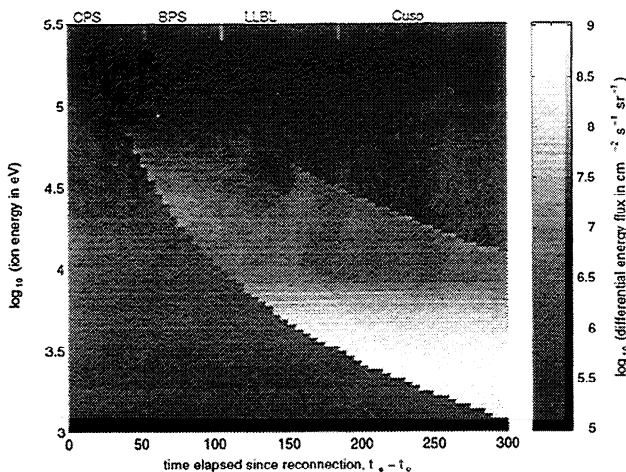

Figure 5. Modeled spectrogram of field-aligned ion precipitation into the ionosphere at the equatorward edge of the cusp region for same conditions as in Figures 3 and 4, with the reconnection site a field-aligned distance of $d = 20\ R_E$ away from the ionosphere. The differential energy flux is grey-scaled as a function of elapsed time since reconnection, $(t_s - t_o)$ and ion energy, using a logarithmic scale. The labels at the top give the precipitation classification, derived using Figure 6.

shown in Figure 4 with the time-of-flight effects was carried out in the manner described by *Lockwood* [1996a]. Figure 5 clearly shows a precipitation of ions with energies up to and exceeding 30 keV which is found immediately equatorward of the cusp. These ions originate from the ri-sp population of sp ions accelerated off the interior Alfvén wave. Their minimum energy falls with larger $(t_s\text{-}t_o)$ because the lower energy ions have time to arrive; the maximum energy falls as the more energetic of the source sp ions are lost because they reach the magnetopause and either are transmitted through it into the magnetosheath or are reflected off it to become part of either the re-sp or ri-sp populations. The first detectable fluxes of magnetosheath ions are seen at about $(t_s\text{-}t_o) = 120$ s, and these are the dominant ions at all energies shown at $(t_s\text{-}t_o) = 300$ s. For a poleward flow speed of 1 km s^{-1}, the first (equatorwardmost) sheath ions will therefore be about 1° poleward of the open-closed boundary.

Note that the accelerated magnetospheric ions share the same dispersion ramp, as seen for BPS ions by *Pinnock et al.* [1993] and for LLBL ions by *Newell et al.* [1991b]. The high-energy ion observations in the boundary regions defined by *Kremser et al.* [1995, Figure 2b] also reveal this feature. By varying the many inputs to the model (Alfvén speeds, densities, temperatures on the two sides of the magnetopause, as well as the reflection and heating factors), model predictions can be produced which readily explain all such examples (not shown here).

5. Evolution of the Precipitation Class With Time Elapsed Since Reconnection

Figure 6 shows the variation of the integral fluxes and average energy in the modeled spectrogram shown in Figure 5, again plotted as a function of elapsed time since reconnection.
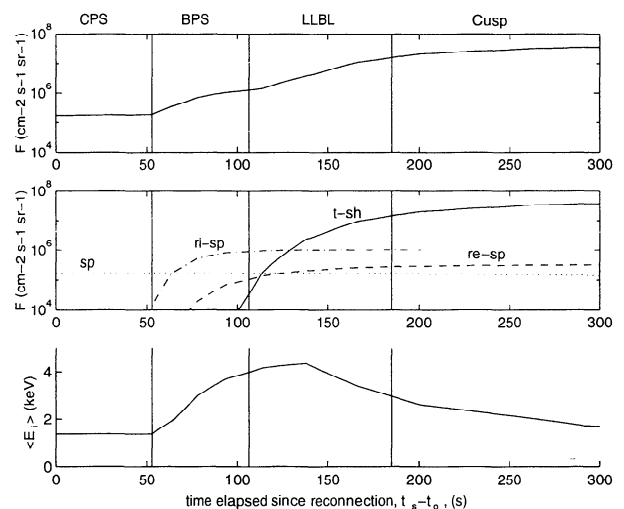
Figure 6. Variations of the integral flux and average energy of the ion populations as a function of elapsed time since reconnection, $(t_s - t_o)$ from the spectrogram in Figure 5. (top) The total integral ion flux in the energy range 30 eV - 30 keV; (middle) The contributions to this total from the ion populations listed in Figure 4, using the same line types (namely dotted line, sp; dotted-dashed line, ri-sp; dashed line, re-sp; and solid line, t-sh); (bottom) The variation of the average ion energy, <E_i>. The regions classified as central plasma sheet (CPS), boundary plasma sheet (BPS), low-latitude boundary layer (LLBL), and cusp (see text) are also shown.

The top graph shows the total integral flux in the 30 eV - 30 keV energy range. The middle graph shows the contributions to this total flux of the various populations (the same line types and labels are employed as in Figure 4). The bottom graph shows the average ion energy.

The question then arises as to how these model populations would be classified in low-altitude satellite observations. Clearly, the sp population is the CPS. The precipitation seen at $(t_s\text{-}t_o) = 300$ s is very similar to the source sheath population and would be classed as cusp. At $(t_s\text{-}t_o) = 190$ s (for our assumed d of 20 R_E), the average ion energy falls below 3 keV, and so prior to this time the definitions used by Newell and Meng [1992, 1994a] would class the precipitation as LLBL. Note that this region is dominated by a mixture of t-sh and ri-sp ions, in other words, a mixture of magnetosheath-like and magnetosphere-like ions which is often thought of as the defining characteristic of the LLBL. Figure 4a shows that ri-sp ions dominate over t-sh at parallel velocities down to $v = 1200$ km s^{-1}. Thus t-sh ions, with flux exceeding that of the ri-sp ions at the same energy, first arrive in the ionosphere at $(t_s\text{-}t_o) = 106$ s, and after this time they will be detected in the ionosphere. This is the boundary between boundary regions 1 and 2 of Kremser et al. [1995] and is here taken to be the time of onset of LLBL precipitation. Immediately prior to this time, the ion distribution is not like that in the CPS region as it has a distinct hot tail and, depending on the electrons, is most likely to be classed as BPS ions. Figure 4 shows that ri-sp ions with phase space density above the one-count level are seen up to a parallel velocity of 2400 km s^{-1} which would arrive in the ionosphere at $(t_s\text{-}t_o) = 53$ s for our assumed d of 20 R_E. However, this time depends critically on the flux of ri-sp ions relative to the one-count level and thus on the density of the source sp ions and the reflection coefficient at the interior wave, r_i. In Figure 4, r_i is equal to 0.03 and reducing it, for example, by a factor of 2 would cause the ri-sp population to be above the one-count level only up to a parallel velocity of 2000 km s^{-1}: thus the ions which cause the onset of the BPS ion classification do not arrive in this case until $(t_s\text{-}t_o) = 64$ s (for the same d of 20 R_E). Reduction of r_i by an order of magnitude would mean that the ri-sp ions would not be seen at all. In such cases, a BPS classification would rest on the detection of sufficient re-sp ions at the higher energies.

In addition, we must consider the behavior of the electrons. The most energetic field-parallel CPS electrons (1 keV - 30 keV) will be lost in the interval of $(t_s\text{-}t_o)$ between 1.2 s and 6.8 s. Thus an abrupt end of energetic CPS electrons is predicted close to the start of the ion dispersion ramp. Some electron fluxes may be maintained by scattering off the magnetopause and by a weak magnetic mirror between the magnetic cusp and the magnetopause [Cowley and Lewis, 1990]. The loss of the CPS electrons may be sufficient to give a "void" classification immediately poleward of the CPS. After ri-sp and/or re-sp ions arrive $(t_s\text{-}t_o > 53$ s in this case), the BPS classification applies in a region across which we would expect any remaining magnetospheric electrons to decay away. However, if the reflection coefficients r_i and r_e are both sufficiently low, the BPS ions will not be seen and the whole region between the CPS and the LLBL would be classed as void. This is one possible reason why the noon BPS is present only 25% of the time in the statistics of Newell and Meng [1992, 1994a].

Figures 5 and 6 clearly demonstrate that the precipitation class evolves with time elapsed since reconnection at the foot of each opened field line as it is transferred from the dayside to the

nightside by the solar wind flow. The boundaries between the regions, as inferred above, are included as vertical lines across each graph in Figure 6 and as short lines at the top of Figure 5. The regions are labeled along the top of both Figures 5 and 6. The evolution from cusp to mantle to polar cap has been understood in terms of the open magnetosphere model, as discussed in the introduction. What is shown here for the first time is that the classification evolves from an initial CPS to BPS to LLBL and to cusp earlier in the same sequence. This evolution is clearly demonstrated in those special cases [e.g. Pinnock et al., 1993; Newell et al., 1991b; Newell and Meng, 1994a] where the satellite path allows it to observe a smooth increase in elapsed time since reconnection (i.e. $(t_s\text{-}t_o)$ increases smoothly with t_s). In many, or even most, cases this will not apply. For example, curved convection streamlines, with the straight satellite orbit path, will distort this variation. However, the greatest effects will be caused by temporal or spatial structure in the reconnection rate, as discussed by Lockwood [1995b] and Lockwood and Davis [1996]. These will both cause discontinuous changes in the observed $(t_s\text{-}t_o)$ and so will be able to generate sharp boundaries, with discontinuous precipitation changes, between the regions.

A second reason for the low BPS occurrence at noon may be that the reconnection is pulsed. From the above, the BPS is seen only after the first arrival of detectable ri-sp ions at $(t_s\text{-}t_o)$ of about 53 s in Figures 5 and 6 and before the arrival of detectable fluxes of t-sh ions at $(t_s\text{-}t_o) = 106$ s. Thus such precipitation lasts for, at most, just 53 s on each newly opened field line. If the reconnection at each MLT were to take place
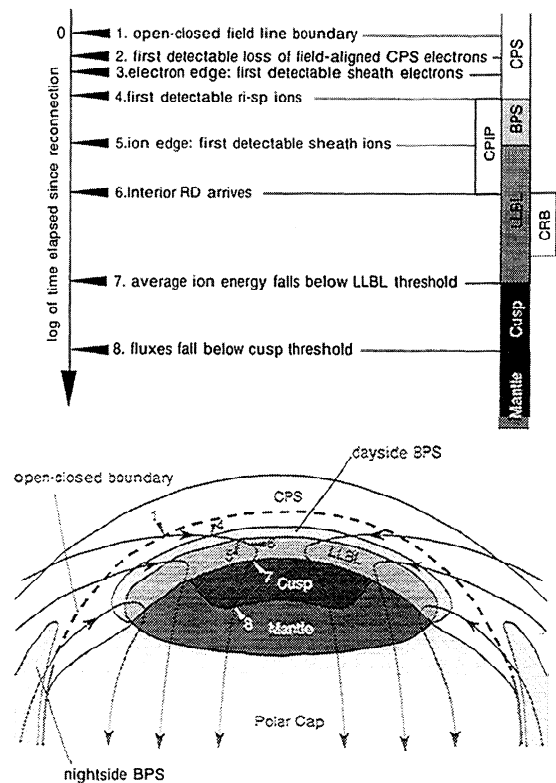
Figure 7. (a) Schematic of the timing of certain events at the foot of each field line as a function of time elapsed since it was reconnected. The coded bar shows the precipitation regions and their relation to the convection reversal boundary (CRB) and the "circum-polar ion precipitation" (CPIP). (b) The same as Figure 1b, but with the events listed in Figure 7 a shown for one example streamline.

only in short pulses (for example, lasting 1 min and repeating every 7 min [see *Lockwood and Davis*, 1995, 1996]), then within each cycle the BPS ions would only be present for the interval between 53 s and (60+106) = 166 s after the start of each pulse. Thus the BPS would be present for only 113 s in each cycle or 27% of the time. In such cases, the LLBL precipitation would appear immediately poleward of the CPS, with a discontinuous step in both ion and electron characteristics at the boundary. This effect would also reduce the occurrence frequency of the LLBL but not by as much because the precipitation lasts for a longer range of elapsed times since reconnection (t_s-t_o between 106 s and 190 s), and the above reconnection rate waveform would give an LLBL occurrence of 34% of the time. The BPS occurrence frequency found by *Newell and Meng* [1994a] at noon is 25%, and this is in a narrow band of latitudes and independent of solar wind dynamic pressure. That for the LLBL is about 20%; however, this applies over a band of latitudes roughly 4° wide for high solar wind dynamic pressure, corresponding to 480 km in the ionosphere. (Presumably, the much lower occurrence rates of LLBL and cusp at low solar wind dynamic pressures reflects the lower solar wind densities, making precipitating fluxes fall below the thresholds for the LLBL and cusp classes; on the other hand BPS, being mainly accelerated magnetospheric ions, is not so affected.) *Newell et al.* [1991a] note that a typical latitudinal width of the LLBL is near 2°. Thus the LLBL occurrence statistics imply an LLBL band (2° wide) is present roughly 40% of the time but that it varies in latitude to give a band of occurrence frequency of 20% which is 4° wide. The cusp and mantle precipitations last for intervals of elapsed time since reconnection which exceeds the period between the reconnection pulses, and so their occurrence frequency is not reduced if the reconnection is pulsed, the main effect being that their latitudinal width is somewhat reduced [*Lockwood and Davis*, 1995].

From the above, we can explain why the dayside BPS population frequently is absent between the CPS and the LLBL in terms of either low reflection factors or as an effect of pulsed reconnection or a mixture of the two. The noon BPS occurrence can be explained entirely in terms of reconnection which comes only in short pulses, but this reduces the LLBL occurrence slightly more than is required to fit the statistical survey of the data, and, in addition, this does not generate a void classification between the CPS and the LLBL. As a result, it is likely that some of the time the fraction of CPS ions which are reflected falls below the threshold value required for the BPS to be seen. Thus we have provided a rationale for including the void region between CPS and LLBL in the schematics of *Newell and Meng* [1994a] as part of the dayside BPS, as was done in Figure 1.

6. Evolution of Each Newly - Opened Field Line and the Patterns of Dayside Precipitation and Flow

The top of Figure 7 shows schematically the important events in the evolution of the precipitations with increasing time elapsed since the field line was reconnected, as discussed above. The first detectable changes, occurring shortly after crossing the open-closed boundary at 1, are the loss of the highest-energy, field-aligned CPS electrons which begin to escape through the magnetopause (at 2) and the arrival of the first detectable fluxes of magnetosheath electrons (at 3). At 4,

detectable fluxes of ri-sp ions arrive, and this marks the boundary between CPS and dayside BPS. When sufficient fluxes of the higher-energy sheath ions begin to arrive and the remnant CPS electrons are gone, the precipitation becomes classed as LLBL. Within the LLBL precipitation region, the interior Alfvén wave (the same wave as that responsible for the ri-sp population) arrives (at 6), and this marks the start of any change in the ionospheric convection flow, that is the equatorward edge of the convection reversal boundary. Note that after the arrival of the first ri-sp ions but before the arrival of the interior wave, the flow is sunward, the ions are more energetic than in the CPS, but the electrons are like those in the polar cap. Thus Figure 7 provides an ideal explanation of *Nishida et al.*'s [1993] classification of "circum-polar ion precipitation" (CPIP) on the dayside. *Newell and Meng* [1994b] argue that these CPIP ions are the LLBL and/or the dayside BPS, which may well be the case, and that the electrons are not exactly the same as in the polar cap, which may also be true. Nevertheless, irrespective of a CPIP or LLBL/BPS classification, Nishida et al. make an important point, namely, that this region is poleward of the electron edge (identified by them as the trapping boundary), and the electrons are much more like those on open field lines within the polar cap than those in the closed CPS. Yet they are convecting sunward and show an energetic ion precipitation [*Nishida and Mukai*, 1994]. This is very well explained by the model reviewed here.

The bottom schematic shows these events on one of the flow streamlines in Figure 1b. This demonstrates how the ionospheric convection reversal boundary (CRB) will generally sit within the LLBL, as was observed by *Newell et al.* [1991a]. The rotation into the polar cap takes place over the broad MLT range of the LLBL, with no need for a throat constriction, and the reconnection takes place over an even broader MLT extent, so the full reconnection voltage does not appear across the cusp region. The precipitation then evolves through the classifications cusp, mantle, and polar cap as expected on newly opened field lines. Note that both the LLBL and the dayside BPS precipitations are on open, not closed, field lines. A clear distinction is made in Figure 7 between nightside and dayside BPS, the former arising from the acceleration of ions in the tail current sheet [see *Onsager and Mukai*, 1995], whereas the latter arise from the interior Alfvén wave at the magnetopause [*Lockwood et al.*, 1996].

This scenario resolves many of the problematic issues discussed in section 3. The flow speed into the polar cap is low because the merging gap is wide and the flow is not restricted to a narrow throat region. The electron edge of energetic magnetospheric electrons appears near the equatorward edge of the BPS, and the open-closed boundary is slightly equatorward of the CPS-BPS boundary. The LLBL and mantle precipitations share roughly the same extent in MLT. That leaves just one additional issue raised in section 3, namely, why is the cusp precipitation seen over a smaller range of MLT than both the LLBL and mantle, if all three are on open field lines?

7. Extent of the Cusp Region

The controlling influences on the dimensions of the cusp are addressed schematically in Figure 8 in terms of a low-latitude reconnection site. The left-hand diagram (Figure 8a) shows the magnetopause, as viewed from the Sun with flow streamlines away from a reconnection X line and circles which are contours of constant sheath density at the magnetopause. These are
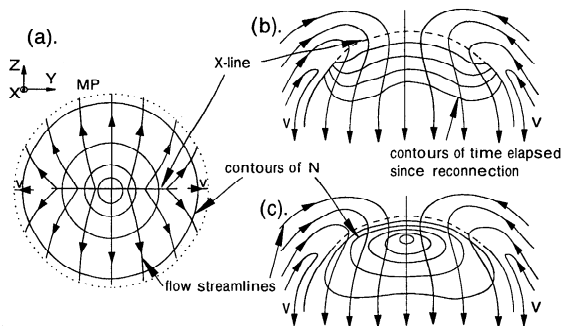
Figure 8. Schematics of cusp precipitation for southward interplanetary magnetic field (IMF). (a) The magnetopause viewed from the sun, showing flow streamlines of newly opened field lines away from a low-latitude reconnection X line and circular contours of magnetosheath plasma density adjacent to the boundary. (b) Resulting flow streamlines and contours of elapsed time since reconnection in the ionosphere. (c) Ionospheric flow and contours of precipitating flux of magnetosheath plasma.

drawn as circular for simplicity, as would be predicted for an axisymmetric gasdynamic model of the magnetosheath [*Spreiter et al.*, 1966]. It can be seen that the field lines reconnected away from the nose of the magnetosphere will sample lower density regions of the sheath than those reconnected near the nose. The previous section discussed how the precipitation characteristics will vary with time elapsed since reconnection $(t_s\text{-}t_o)$, contours of which are shown schematically in Figure 8b. The variation of flux along each flow streamline in the ionosphere will also reflect the variation of the density of the source magnetosheath plasma along the corresponding flow streamline on the magnetopause. This gives a variation in flux with longitude, as well as latitude, as shown in Figure 8c. As the definition of cusp requires that there be sufficient energy flux carried by the particles yet that the average energy is sufficiently low; the cusp appears over a smaller MLT range near noon than the LLBL and mantle precipitations and than the merging gap. At MLT closer to dawn or dusk, the classification evolves directly from LLBL to mantle.

These ideas can be used to make quantitative predictions for how the cusp extent, in both longitude and latitude, will vary with solar wind density. These predictions are shown in Figures 9 and 10. They are based on the criteria devised by *Newell and Meng* [1992] that the integral energy flux must exceed 10^{10} eV cm^{-2} s^{-1} sr^{-1}, but the average energy must be less than 3 keV in order for the precipitation to be classed as cusp.

Figure 9a shows how the density of magnetosheath plasma adjacent to the equatorial magnetopause, N_{sh}, varies with the separation in MLT from the nose of the magnetosphere. In this plot, N_{sh} is shown as a ratio of the upstream solar wind value N_{sw} and is taken from the gasdynamic modeling of *Spreiter et al.* [1966]. If we consider that N_{sh} has to be over some threshold value in order to give integral energy fluxes into the ionosphere which are large enough to be classed as cusp, yet an average energy low enough to avoid an LLBL classification, then we can compute the MLT extent of the segment of the magnetopause which can contribute to the cusp. This is shown in Figure 9b as a function of the ratio (N_{sw}/N_{th}), where N_{th} is the threshold value of N_{sw} required for those open field lines generated at the nose of the magnetosphere to produce precipitation of sufficient energy flux to be classed as cusp. This

normalization means that the predictions are valid for any other definition of the threshold cusp flux. Because of its linear dependence on solar wind density, the (normalized) solar wind dynamic pressure (P_{sw}) would have a corresponding effect.

The magnetic mapping of the MLT extent shown in Figure 9b to the ionospheric cusp will be complex and has been predicted to depend on the reconnection voltage. *Crooker et al.* [1991] modeled the length of the merging gap, the ionospheric footprint of a reconnection X line which spanned a fixed length of roughly 15.5 hours of MLT along the equatorial magnetopause: their Figure 5 indicates that the ionospheric projection of such an X line increases from about 4 to 6 hours of MLT as the voltage increases from a moderate (for southward IMF conditions) 50 kV to a very large value of 170 kV. If we consider the effect at a constant voltage near 100 kV, the 15.5 hours on the magnetopause maps to 5 hours in the ionosphere, a factor of about 3.

There is one statistical survey of observations which can be used as a first-order test of these predictions. *Newell and Meng* [1994] found that the cusp width was 2 and 4 hours of MLT for cases in which $P_{sw} < 2$ nPa and $P_{sw} > 4$ nPa, respectively. For these two subsets of the data, the mean values were $<N_{sw}> = 5.5$ cm^{-3}, $<P_{sw}> = 1.5$ nPa , and $<V_{sw}> = 428.8$ km s^{-1} and $<N_{sw}> = 17.7$ cm^{-3}, $<P_{sw}> = 6.0$ nPa , and $<V_{sw}> = 478$ km s^{-1}. Thus these statistics imply that tripling the solar wind density will double the cusp width (neglecting any effects associated with the difference between the $<V_{sw}>$ for the two cases): this is broadly consistent with the behavior predicted in Figure 9b, all other factors being constant, provided N_{sw} does not approach the threshold value, N_{th}. Using the approximate (and constant) MLT mapping factor of 3 from the work of Crooker et al. (see above), the two data subsets give magnetopause source extents of about 6 and 12 hours, respectively; these are consistent with Figure 9b, if N_{th} is of the order of 2.5 cm^{-3}. From the ratio of the peak integral energy flux predicted by the cusp model by *Lockwood* [1995a] to the
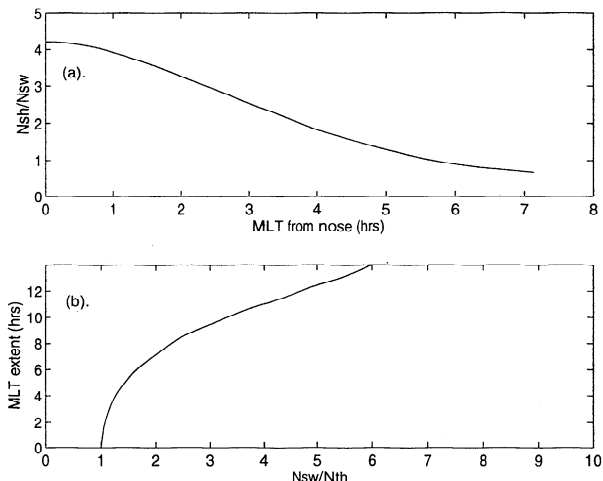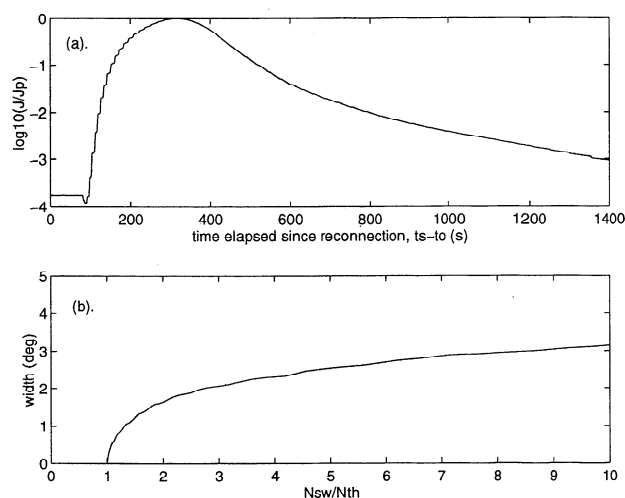

Figure 9. The prediction of the variation of cusp longitudinal extent as a function of solar wind density using the gas dynamic magnetosheath model of *Sprieter et al.*[1966]. (a) The ratio of magnetosheath density divided by the solar wind value, (N_{sh}/N_{sw}), as a function of the separation in MLT from the nose of the magnetosphere. (b) The MLT extent of that part of the magnetopause contributing to cusp precipitation region, as a function of N_{sw}, given as a ratio of its threshold value N_{th} (see text for details).

threshold cusp energy flux of 10^{10} eV cm^{-2} s^{-1} sr^{-1} used by *Newell and Meng* [1992, 1994a], we can estimate N_{th} is of the order of 2 cm^{-3}. This value is also consistent with the statistical survey of *Aparicio et al.* [1991]: their Figure 5 shows that cusp observations were made for N_{sw} values down to a lower limit of N_{th} = 2 cm^{-3}. From the above, although there will be complications introduced by variations of the magnetic mapping (from the magnetopause to the ionosphere), the observed variation of cusp width with dynamic pressure is broadly consistent with the concept of the ionospheric reconnection merging gap being longer than the cusp. The longitudinal width of the cusp is set by, and varies with, the solar wind density by virtue of the longitudinal variation of the magnetosheath density.

Similarly, Figure 10 predicts the variations in the latitudinal width of the cusp. Figure 10a shows the integral precipitating energy flux J, predicted by the model [see *Lockwood*, 1995a] as a ratio of its peak value and as a function of time elapsed since reconnection $(t_s\text{-}t_o)$. The cusp/LLBL boundary is where the mean ion energy falls below 3 keV and does not depend on N_{sw}. On the other hand, the cusp/mantle boundary is where the energy flux falls below 10^{10} eV cm^{-2} s^{-1} sr^{-1} and will move poleward as N_{sw} increases. By comparison with the threshold condition used by *Newell and Meng* [1992, 1994a] and by adopting a steady poleward convection speed of 1 km s^{-1}, we can use Figure 10a to predict the variation of cusp width with the ratio (N_{sw}/N_{th}). This is shown in Figure 10b. Using the N_{th} of 2 cm^{-3} inferred above, the mean values of the two data subsets of *Newell and Meng* [1994a] ($<N_{sw}>$ of 5.5 cm^{-3} and 17.7 cm^{-3}) give predicted cusp widths of 2° and 3°. These are roughly consistent with the results of Newell and Mengs's cusp survey. This implies that cusp latitudinal width, like its longitudinal extent, is controlled by the solar wind density by a threshold effect.

8. Conclusions

This paper has used the explanation of *Lockwood et al.* [1996] of the acceleration of dayside BPS ions equatorward of

the cusp. The model gives the framework for a unified explanation of all the dayside precipitation regions during southward IMF. The precipitation at the foot of each newly opened field line is predicted to evolve from the initial CPS population, present prior to reconnection on closed field lines, to BPS (or void), LLBL, cusp, mantle, and then to polar cap. The precipitations on newly opened field lines share a common dispersion ramp in energies, as has been observed when conditions are right (specifically, for quasi-steady reconnection and a satellite whose path maintains a relatively constant orientation with the flow streamline). Low magnetospheric densities may cause CPS to be classed as void and this and/or a low reflection coefficient at the Alfvén waves may cause BPS to also be classed as void. In addition, the low occurrence probabilities of BPS and LLBL precipitations near noon found by *Newell and Meng* [1994a] suggest that a fully pulsed reconnection rate may also be a factor. Such pulses, and/or spatial structure in the reconnection rate, along with the pattern of convective flow, will generate discontinuous steps in the precipitation which will often sit on the boundaries between the precipitation regions. The densities in the sheath mean that the precipitation only has sufficient density to be classed as cusp near noon.

This model can, at least qualitatively, explain the extents in MLT over which various precipitation classes are seen (section 3.1). Its use means that there is no need for the predominantly reconnection-driven flow to be constricted to a narrow convection throat in the cusp ionosphere (see section 3.2) with unrealistically high flows there. We have also placed the open-closed boundary in a location which does not give rise to severe paradoxes when we consider the dispersion of particles across that boundary by convection (section 3.3) and which places the observed electron edge in the correct location (section 3.4). The model also explains the location of the dayside convection reversal boundary in relation to the precipitations and provides an unique explanation of the observations of circumpolar ion precipitation on sunward convecting open field lines.

Figure 10. The prediction of the latitudinal width of the cusp using the ion injection, acceleration, and transport model of *Lockwood* [1995a]. (a) Model predictions of the variation of integral energy flux of ions as a function of elapsed time since reconnection $(t_s\text{-}t_o)$. (b) Variation of cusp latitudinal width (for a fixed poleward convection speed of 1 km s^{-1}) as a function of (N_{sw}/N_{th}).

References

Alem, F., and D.C. Delcourt, Nonadiabatic precipitation of ions at the cusp equatorward edge, *J. Geophys. Res., 100*, 19,321, 1995.

Aparicio, B., B. Thelin, and R. Lundin, The polar cusp from a particle point of view: A statistical model based on Viking data, *J. Geophys. Res., 14,023*, 1991.

Baker, K.B., A.S. Rodger, and G. Lu, HF-radar observations of the dayside magnetic merging rate: A GEM boundary layer campaign study, *J. Geophys. Res., 102*, 9603, 1997.

Burch, J. L., Quasi-neutrality in the polar cusp, *Geophys. Res. Lett., 12*, 469-472, 1985.

Cowley, S.W.H., Magnetospheric asymmetries associated with the Y-component of the IMF, *Planet Space Sci., 29*, 79, 1981.

Cowley, S.W.H., The causes of convection in the Earth's magnetosphere: A review of developments during IMS, *Rev. Geophys., 20*, 531-565, 1982.

Cowley, S.W.H., Solar wind control of magnetospheric convection, in *Achievements of the International Magnetospheric Study, IMS, Eur. Space Agency Spec Publ., ESA SP-217*, 483-494, 1984.

Cowley, S.W.H., and Z.V. Lewis, Magnetic trapping of energetic particles on open dayside boundary layer flux tubes, *Planet. Space Sci., 38*, 1343, 1990.

Cowley, S.W.H., and M. Lockwood, Excitation and decay of solar wind-driven flows in the magnetosphere-ionosphere system, *Ann. Geophys., 10*, 103-115, 1992.

Cowley, S.W.H., D.J. Southwood, and M.A. Saunders, Interpretation of magnetic field perturbations in the Earth's magnetopause boundary, *Planet. Space Sci., 31*, 1237, 1983.

Cowley, S.W.H., J.P. Morelli, and M. Lockwood, Dependence of convective flows and particle precipitation in the high-latitude dayside ionosphere on the *X* and *Y* components of the interplanetary magnetic field, *J. Geophys. Res., 96*, 5557, 1991a.

Cowley, S.W.H., M.P. Freeman, M. Lockwood, and M.F. Smith, The ionospheric signature of flux transfer events, in *"CLUSTER - Dayside Polar Cusp"*, edited C.I. Barron, *Eur. Space Agency Spec. Publ., ESA SP-330*, 105-112, 1991b.

Crooker, N.U., F.R. Toffoletto, and M.S. Gussenhoven, Opening the cusp, *J. Geophys. Res., 96*, 3497, 1991.

Curran, D.B., and C.K. Goertz, Particle distributions in a two-dimensional reconnection field geometry, *J. Geophys. Res., 94*, 272, 1989.

Daly, P.W., and T.A. Fritz, Trapped electron distributions on open field lines, *J. Geophys. Res., 87*, 6081, 1982.

de la Beaujardiere, O., P. Newell, and R. Rich, Relationship between Birkeland current regions, particle participation, and electric fields, *J. Geophys. Res., 98*, 7711, 1993.

Eastman, T.E., and E.W. Hones Jr., Characteristics of the magnetospheric boundary layer as observed by IMP - 6, *J. Geophys. Res., 84*, 2109, 1979.

Eastman, T.E., E.W. Hones Jr., S.J. Bame, and J.R. Ashbridge, The magnetospheric boundary layer: Site of plasma, momentum and energy transfer from the magnetosheath to the magnetosphere, *Geophys. Res. Lett., 3*, 685-688, 1976.

Fuselier, S.A., D.M. Klumpar, and E.G. Shelley, Ion reflection and transmission during reconnection at the Earth's subsolar magnetopause, *Geophys. Res. Lett., 18*, 139, 1991.

Gosling, J.T., M.F. Thomsen, S.J. Bame, R.C. Elphic, and C.T. Russell, Plasma flow reversals at the dayside magnetopause and the origin of asymmetric polar cap convection, *J. Geophys. Res., 95*, 8073, 1990a.

Gosling, J.T., M.F. Thomsen, S.J. Bame, T.G. Onsager, and C.T. Russell, The electron edge of the low-latitude boundary layer during accelerated flow events, *Geophys. Res. Lett., 17*, 1833-1836, 1990b.

Hapgood, M.A., and D.A. Bryant, Exploring the magnetospheric boundary layer, *Planet Space Sci., 40*, 1431, 1992.

Heelis, R.A., W.B. Hanson, and J.L. Burch, Ion convection reversals in the dayside cleft, *J. Geophys. Res., 81*, 3803, 1976.

Heppner, J.P. and N. C. Maynard, Empirical high-latitude electric field models, *J. Geophys. Res., 92*, 4467, 1987.

Hill, T.W., and P.H. Reiff, Evidence of magnetospheric cusp proton acceleration by magnetic merging at the dayside magnetopause, *J. Geophys. Res., 82*, 3623, 1977.

Jørgensen, T.S., E. Friis-Christiansen, V.B. Wickwar, J.D. Kelly, C.R. Clauer, and P.M. Banks, On the reversal from "sunward" to "antisunward" plasma convection in the dayside high latitude ionosphere, *Geophys. Res. Lett., 1*, 887-890, 1984.

Kremser, G., J. Woch, K. Mursala, P. Tanskanen, B. Wilken, and R. Lundin, Origin of energetic ions in the polar cusp inferred from ion composition measurements by the Viking satellite, *Ann. Geophys., 13*, 595-607, 1995.

Lockwood, M., On flow reversal boundaries and cross-cap potential in average models of high latitude convection, *Planet. Space Sci., 39*, 397, 1991

Lockwood, M., The location and characteristics of the reconnection X-line deduced from low-altitude satellite and ground-based observations, 1, Theory, *J. Geophys. Res., 100*, 21,791, 1995a.

Lockwood, M., Ground-based and satellite observations of the cusp: Evidence for pulsed magnetopause reconnection, in *Physics of the Magnetopause, Geophys. Monogr. Ser.*, vol. 90, edited by P.Song, B.U.O. Sonnerup and M.F. Thomsen, pp. 417-426, AGU, Washington, D.C., 1995b.

Lockwood, M., and C.J. Davis, The occurrence probability, width and number of steps of cusp precipitation for fully - pulsed reconnection at the dayside magnetopause, *J. Geophys. Res., 100*, 7627, 1995.

Lockwood, M., and C.J. Davis, On the longitudinal extent of magnetopause reconnection bursts, *Ann. Geophys., 14*, 865-878, 1996.

Lockwood, M., and J. Moen, Ion populations on open field lines within the day-side low-latitude boundary layer: Theory and observations during a transient event, *Geophys. Res Lett., 23*, 2895-2893, 1996.

Lockwood, M., and M.F. Smith, Comment on "Mapping the dayside ionosphere to the magnetosphere according to particle precipitation characteristics" by Newell and Meng, *Geophys. Res. Lett., 20*, 1739-1740, 1993.

Lockwood, M., and M.F. Smith, Low and middle-altitude cusp particle signatures for general magnetopause reconnection rate variations, I, Theory, *J. Geophys. Res., 99*, 8531, 1994.

Lockwood, M., W.F. Denig, A.D. Farmer, V.N. Davda, S.W.H. Cowley, and H. Lühr, Ionospheric signatures of pulsed magnetic reconnection at the Earth's magnetopause, *Nature, 361*, 424-428, 1993.

Lockwood, M., T.G. Onsager, C.J. Davis, M.F. Smith, and W.F Denig, The characteristics of the magnetopause reconnection X-line deduced from low-altitude satellite observations of cusp ions, *Geophys. Res. Lett., 21*, 2757-2760, 1994.

Lockwood, M., S.W.H. Cowley, and T.G. Onsager, Ion acceleration at both the interior and exterior Alfvén waves associated with the magnetopause reconnection site: signatures in cusp precipitation, *J. Geophys. Res., 101*, 21,501, 1996.

Lotko, W., and B.U.O. Sonnerup, The low-latitude boundary layer on closed field lines, in *Physics of the Magnetopause, Geophys. Monogr. Ser.*, vol. 90, edited P. Song, B.U.O. Sonnerup, and M. Thomsen, pp. 371-383, AGU Washington, D.C., 1995.

Lyons, L.R., M. Schulz, D.C. Pridmore-Brown, and J.L. Roeder, Low-latitude boundary layer near noon: An open field line, *J. Geophys. Res., 99*, 2227, 1994.

Mitchell, D.G., F. Kutchko, D.J. Williams, T.E. Eastman, L.A. Frank, and C.T. Russell, An extended study of the low-latitude boundary layer on the dawn and the dusk flanks on the magnetosphere, *J. Geophys. Res., 92*, 7394, 1987.

Moen, J., D. Evans, H.C. Carlson, and M. Lockwood, Dayside moving auroral transients related to LLBL dynamics, *Geophys. Res. Lett., 23*, 3247-3250, 1996

Newell, P.T., and C.-I. Meng, Mapping the dayside ionosphere to the magnetosphere according to particle precipitation characteristics, *Geophys. Res. Lett., 19*, 609-612, 1992.

Newell, P.T., and C.-I. Meng, Reply, *Geophys. Res. Lett., 20*, 1741-1742, 1993.

Newell, P.T., and C.-I. Meng, Ionospheric projections of magnetospheric regions under low and high solar wind pressure conditions, *J. Geophys. Res., 99*, 273, 1994a.

Newell, P.T., and C.-I. Meng, Comment on "Unexpected features of the ion precipitation in the so-called cleft/low latitude boundary layer region: Association with sunward convection and occurrence on open field lines" by A. Nishida, T. Mukai, H. Hayakawa, A. Matsuoka, K. Tsuruda, N. Kaya, and H. Fukunishi, *J. Geophys. Res., 99*, 19,609, 1994b.

Newell, P.T., W.J. Burke, E.R. Sanchez, C.-I. Meng, M.E. Greenspan, and C.R. Clauer, The low-latitude boundary and the boundary plasma sheet at low altitude: Prenoon precipitation regions and convection reversal boundaries, *J. Geophys. Res., 96*, 21,013, 1991a.

Newell, P.T., W.J. Burke, C.-I. Meng, E.R. Sanchez, and M.E. Greenspan, Identification and observation of the plasma mantle at low altitude, *J. Geophys. Res., 96*, 35, 1991b.

Nishida, A., Can random reconnection on the magnetopause produce the low-latitude boundary layer?, *Geophys. Res. Lett., 16*, 227-230, 1989.

Nishida, A., and T. Mukai, Reply to comment on "Unexpected features of the ion precipitation in the so-called cleft/low-latitude boundary layer region" by A. Nishida et al., *J. Geophys. Res., 99*, 23,367, 1994.

Nishida, A., T. Mukai, H. Hayakawa, A. Matsuoka, and K. Tsuruda, Unexpected features of the ion precipitation in the so-called cleft/low-latitude boundary layer region: Association with sunward convection and occurrence on open field lines, *J. Geophys. Res., 98*, 11,161, 1993.

Ohtani, S.-I., et al., Four large-scale field-aligned current systems in the dayside high-latitude region, *J. Geophys. Res., 100*, 137, 1995a.

Ohtani, S.-I., T.A. Potemra, P.T. Newell, L.J. Zanetti, T. Iijima, M.

Wantanabe, M. Yamauchi, R.D. Elphinstone, O. de la Beaujardiére, and L.G. Blomberg, Simultaneous prenoon and postnoon observations of three field-aligned current systems from Viking and DMSP-F7, *J. Geophys. Res.*, *100*, 119, 1995b.

Onsager, T.G., and T. Mukai, Low altitude signature of the plasma sheet boundary layer: Observations and model, *Geophys, Res. Lett.*, 22, 855-858,1995.

Onsager, T.G., C.A. Kletzing, J B. Austin, and H. MacKiernan, Model of magnetosheath plasma in the magnetosphere: Cusp and mantle precipitations at low altitudes, *Geophys. Res. Lett.*, *20*, 479-482, 1993.

Owen, C.J. and J.A. Slavin, Viscously driven plasma flows in the deep geomagnetic tail, *Geophys. Res. Lett.*, *19*, 1443-1446, 1992.

Paschmann, G., I. Papamastorakis, W. Baumjohann, N. Sckopke, C.W. Carlson, B.U.Ö. Sonnerup, and H. Lühr, The magnetopause for large magnetic shear: AMPTE/IRM observations, *J. Geophys. Res.*, *91*, 11099, 1986.

Pinnock, M., A.S. Rodger, J.R. Dudeney, K.B. Baker, P.T. Newell, R.A. Greenwald, and M.E. Greenspan, Observations of an enhanced convection channel in the cusp ionosphere, *J. Geophys. Res.*, *98*, 3767, 1993.

Reiff, P.H., T.W. Hill, and J.L. Burch, Solar wind plasma injection at the dayside magnetospheric cusp, *J. Geophys. Res.*, *82*, 479, 1977.

Richard, R.L., R.J. Walker, and M. Ashour-Abdalla, The population of the magnetosphere by solar wind ions when the interplanetary magnetic field is northward, *Geophys. Res. Lett.*, *21*, 2455-2458, 1994.

Scholer, M., P.W. Daly, G. Paschmann, and T.A. Fritz, Field line topology determined by energetic particles during a possible magnetopause reconnection event, *J. Geophys. Res.*, *87*, 6073, 1982.

Shue, J.-H., and D.R. Weimer, The relationship between ionospheric convection and magnetic activity, *J. Geophys. Res.*, *99*, 401, 1994.

Siscoe, G.L., and T.S. Huang, Polar cap inflation and deflation, *J. Geophys. Res.*, *90*, 543, 1985.

Smith, M.F., and D.J. Rodgers, Ion distributions at the dayside magnetopause, *J. Geophys. Res.*, *96*, 11,617, 1991.

Song, P., and C.T. Russell, Model of the formation of the low-latitude boundary layer for strongly northward interplanetary magnetic field, *J. Geophys. Res.*, *97*, 1411, 1992.

Song, P., R.C. Elphic, C.T. Russell, J.T. Gosling, and C.A. Cattell, Structure and properties of the subsolar magnetopause for northward IMF: ISEE observations, *J. Geophys. Res.*, *95*, 6375, 1990.

Sonnerup, B.U.Ö., Theory of the low-latitude boundary layer, *J. Geophys. Res.*, *85*, 2017, 1980.

Sonnerup, B.U.Ö., I. Papamastorakis, G. Paschmann, and H,.Lühr, The magnetopause for large magnetic shear: Analysis of convection electric fields from AMPTE/IRM, *J. Geophys. Res.*, *95*, 10541, 1990.

Spreiter, J.R. A.L. Summers, and A.Y. Alksne, Hydromagnetic flow around the magnetosphere, *Planet. Space Sci.*, *14*, 223, 1966.

Stasiewicz, K., Polar cusp topology and position as a function of interplanetary magnetic field and magnetic activity: comparison with Viking and other observations, *J. Geophys. Res.*, *96*, 15789, 1991.

Traver, D.P., D.G. Mitchell, D.J. Williams, L.A. Frank, and C.Y. Huang, Two encounters with the flank low-latitude boundary layer: further evidence for closed field line topology and investigation of internal structure, *J. Geophys. Res.*, *96*, 21,025, 1991.

Treumann, R.A., J. LaBelle, and T.M. Bauer, Diffusion processes: An observational perspective, in *Physics of the Magnetopause*, *Geophys. Monogr. Ser,.* vol. 90, edited P. Song, B.U.Ö. Sonnerup, and M. F. Thomsen, pp. 331-341, AGU Washington, D.C., 1995.

Vasyliunas, V.M., Interaction between the magnetospheric boundary layers and the ionosphere, in *Proceedings of the Magnetospheric Boundary Layers Conference, Alpbach, Eur. Space Agency Spec Publ., ESA SP-148*, 387-394, 1979.

Watermann, J., O. de la Beujardiére, and H.E. Spence, Space-time structure of the morning aurora inferred from coincident DMSP-F6,-F8, and Sondrestrom incoherent scatter radar observations, *J. Atmos. Terr. Phys.*, *55*, 1728-1739, 1993.

Winske, D., V.A. Thomas, and N. Omidi, Diffusion at the magnetopause: A theoretical perspective, in *Physics of the Magnetopause, Geophys. Monogr Ser.*, vol. 90, edited P. Song, B.U.Ö. Sonnerup, and M. F. Thomsen, pp. 321-330, AGU, Washington, D.C., 1995.

Woch, J., and R. Lundin, Magnetosheath plasma precipitation in the polar cusp and its control by the interplanetary magnetic field, *J. Geophys. Res.*, *97*, 1421, 1992.

Woch, J., and R. Lundin, The low-latitude boundary layer at mid-altitudes: Identification based on Viking hot plasma data, *Geophys. Res. Lett.*, *20*, 979-982, 1993.

M. Lockwood, Rutherford Appleton Laboratory, Chilton, Oxon, OX11 0QX, England, UK. (e-mail: m.lockwood@rl.ac.uk)